International Journal of Science and Research (IJSR)
ISSN: 2319-7064
SJIF (2022): 7.942

Uniform Haar Wavelet Scheme for the Approximate Solution of System of Partially Singularly Perturbed Problems on Non-Uniform Grid

Aditya Sharma* and Late Manoj Kumar

Department of Mathematics, Motilal Nehru National Institute of Technology Allahabad, Prayagraj-211004, India

Email: adityas@mnnit.ac.in

Abstract:

The purpose of this paper is to present a uniform Haar wavelet method for approximating the solution of a system of partially singularly perturbed problems numerically. The approximate solution is considered on non-uniform grids. Linear and second-order system of partially singularly perturbed problems are considered for different meshes to reduce the issues of singular behavior and provides an approximate solution up to the specified order. By performing the computation on present numerical algorithm, our scheme produces better results than the non-uniform method, the parameter uniform method, and the classical finite difference operator method. The approach is shown to be uniformly convergent in terms of the singular perturbation parameter and error estimation. The effectiveness of the present scheme is examined through some test examples.

Keywords: Differential Equation System; Uniform Haar Wavelet Method; Singular Perturbation; Initial and Boundary Value Problem; Convergence and Error Analysis.

AMS Subject Classification: 34D15; 65L11; 65H10

*Corresponding Author

1 Introduction

The primary goal of this article is to describe a specific case of a system of partially singularly perturbed problem with a small perturbation parameter ε in one equation. Here, the class of linear and second order system of singularly perturbed (SP) initial and boundary value problems (BVP)as below:

$$\varepsilon u_1'(x) + \alpha_0 u_1(x) + \alpha_1 u_2(x) = r_1(x), \quad (1)$$

$$u_2'(x) + \alpha_2 u_1(x) + \alpha_3 u_2(x) = r_2(x), \ \forall x \in (0, 1], \quad (2)$$

with initial conditions:

$$u_1(0) = a_1, \quad u_2(0) = a_2, \quad (3)$$

and,

$$-\varepsilon u_1''(x) + \alpha_0 u_1(x) + \alpha_1 u_2(x) = r_1(x), \quad (4)$$

$$u_2''(x) + \alpha_2 u_1(x) + \alpha_3 u_2(x) = r_2(x), \ \forall x \in (0, 1], \quad (5)$$

with respect to boundary conditions:

$$u_1(0) = a_1, \ u_2(0) = a_2, \ u_1(1) = a_3 \text{ and } u_2(1) = a_4. \quad (6)$$

Perturbation parameter associated in the singularly perturbed problems (SPPs) is relatively a small parameter: $\varepsilon \ll 1$. The small perturbation parameter ε, ($0 < \varepsilon \ll 1$) multiplied with the highest differential operator in the system of first order (initial value) and second order boundary value problems with partial singular perturbations. Perturbation parameter leads to the change in the behavior of the Haar solution to the corresponding singularly perturbed initial value problems (SPIVPs). It is generally known that SPP frequently features interior layers with thin boundary layers and layers where the solution varies quickly., yet away from the layers, solution behaves regularly and varies slowly. x is an independent variable, The functions $u_i(x)$ for i=1,2,3,4 is unknown. Which are continuous and differentiable on an interval [0, 1] of the real number axis x, α_i for i = 1, 2, 3, 4 are the constant coefficients, $r_1(x), r_2(x)$ are given functions of the independent variable x. Further assume that the functions $r_1(x), r_2(x), u_i(x), i = 1, 2, 3, and\ 4$ with the coefficients α_i for i = 1, 2, 3, 4 takes the real values. The following systems can be found in a variety of fields, including radiology, biophysics, chemical reactions, psychology, semiconductor inputs, neurosciences, circuit study, geophysics, diffusion processes, pattern reorganization problems, and mathematical miniatures in water waves. The study of diffusion process generated by chemical reaction is one use of this system of linear singularly perturbed boundary value problems (SPBVPs) in electro-analytic chemistry, combustion theory, semiconductor devices, heat transfer, semiconductor modelling, optimal control, and hydrodynamics. The diffusion coefficient of the substances is defined by small parameters multiplied with the highest derivatives.

For the study of systems of partially singularly perturbed problems authors refer (Lambert (1991) and Doolan et al., 1980). For extensive study of such problems, various schemes have been developed, such as Matthews et al., (Matthews et al., 2006) gave a parameter-uniform numerical technique with asymptotic convergence independent of singular perturbation parameters, The system of several novel methods for somewhat singularly perturbed initial and boundary value issues is addressed in (Das et al., 2017, Umesh and Kumar (2020) and Kumar and Deswal (2021) explained the numerical approach using wavelets to solve two-point SPPs. Singh et. al., (2023) solved fourth order SPBVPs via uniformly convergent scheme.

However, for a system of singularly perturbed concerns, there are just a few results given in the literature. Therefore, in this paper, piece-wise Shishkin mesh, p-mesh and q-mesh are considered to solve the system of linear initial and BVPs that are slightly singularly perturbed. Uniform Haar wavelet scheme has been taken to solve the linear system of initial and second order system of partially SPBVPs. Furthermore, uniform Haar wavelet methodology outperforms parameter uniform methods, non-uniform methodology and traditional numerical difference operator theory, and demonstrated the uniform Haar wavelet method's better efficiency with two test problems. The structure of this research is as follows: The Uniform Haar Wavelet Method (UHWM) and its integrals has been described in Section 2. The method of the approximation function for the Haar wavelet is described in the next section. The piece-wise non-uniform fitted mesh/grids are defined and suggests a numerical technique for the system of singularly perturbed initial (first order) and boundary value (second order) is given in section 4. Section 5 gave convergence analysis and error analysis of the present method. Section 6 discusses the findings and conclusions as to demonstrate the suggested method's correctness, and validity. Finally, section 7 provides a summary of the paper's conclusions.

2 Uniform Haar Wavelet Method

Chen and Hsiao (1997) developed the Haar Wavelet Method (HWM) for the solution of parametric systems with lumped and distributed parameters, which is a fully distributed model that takes into account fluid property fluctuation. Following a series of papers studied by Lepik (2011). Haar wavelets are gaining prominence in the field of differential equations. Many researchers were drawn to Haar wavelet-based approaches because of their accuracy, low processing cost, and superiority to alternative numerical methods. Researchers were drawn to

new ideas in Lepik and Hein (2014), (Singh at al., 2019), (Swati at al., 2020), and (Islam et al., 2010). In this study, a partial system of singularly perturbed initial/boundary value problems is numerically solved using the wavelets approach. The following are the major features of Haar wavelets that are relevant in numerical findings:

- The Haar basis function's complexity allows for an approach to creating a set of solutions while requiring less time and calculation.
- It's computationally convenient method that uses constructive algorithms to manage a numerous initial and boundary conditions.

2 Uniform Haar Wavelet Method and their integrals

Approximation of any square integrable function at different levels of resolution discussed in Lepik (2008) and Clavero and Jorge (2016), The mother wavelet is a great wavelet-based effort that incorporates translation and dilation of signal function and defined over the given interval x belongs to [A, B] as follows:

$$h_i^W(x) = \{\ 1,\ -1,\ 0,\quad if\quad \vartheta_1(i) \leq x < \vartheta_2(i)\ \ if\ \vartheta_2(i) \leq x < \vartheta_3(i)\ elsewhere$$

Where:

$$\vartheta_1 = \frac{k}{m},\quad \vartheta_2 = \frac{2k+1}{2m},\quad \vartheta_3 = \frac{k+1}{m},$$

where i=

2^{j+k+1}, $\vartheta_1(i) = A + 2k\mu\Delta x,\ \vartheta_2(i) = A + (2k+1)\mu\Delta x,\ \vartheta_3(i) = A2(k+1)\mu\Delta x,\ \mu = \frac{M}{m},$

and $\Delta x = \frac{B-A}{2M}$, For the value of i=1, Haar function $h_i^W(x)$ is the scaling parameter function for family of Haar wavelets and is described as:

$$h_1^W(x) = \{\ 1,\quad if\ \ 0 \leq x < 1\ 0,\qquad elsewhere \tag{8}$$

$$\int_0^1 h_i^W(x)\, h_l^W(x) =$$

$$\{\ 2^{-j},\quad if\ i = l = k + 2^j\ 0,\qquad elsewhere \tag{9}$$

for $i = 2$, the function $h_2^W(x)$ is known as the mother wavelet for the family of Haar wavelet, and is described as

$$h_2^W(x) = \{\ 1,\ -1,\ 0,\quad if\quad \vartheta_1(i) \leq x < \vartheta_2(i)\ \ if\ \vartheta_2(i) \leq x < \vartheta_3(i)\ elsewhere$$

Here, the integer m=2^j $with\ j = 0, 1, 2 \ldots J,$ parameter k=0,1,2…, m-1. Consider a minimum index of i=1 for the Haar function, select m=1, k=0. The highest value that the index number can takes i=2M= 2^{j+1}, if wavelet every level is included. Parameter, J represents the maximum level of resolution. The highest degree at which uniform Haar solutions are computed using the numerical analysis algorithm. The highest resolution signifies the most accurate approximation of Haar solution. The Parameter (J) usually associated with the index of the Haar function.

In addition, $h_2^W(x)$ is the mother Haar wavelet, which spans the full range (0,1), or the fundamental square wave. Similar to this, all future curves are produced using the Haar wavelet algorithm utilizing two operations: dilation and translation followed by Raza and Khan (2021).

The Haar operational matrices of integration will then use to calculate the numerical solution to the system of partially SPPs.

The operational matrix $P_{i,ς}$ for Haar of order of order $m \times m$ is created by integrating the Haar wavelet family using the integral as the basis and defined as below:

$$P_{i,ς} = \int_A^x \int_A^x \ldots\ldots\ldots \int_A^x h_i^w(t)dt^ς = \frac{1}{(ς-1)} \int_A^x (x - t)^{ς-1} h_i^w(t)dt, \qquad (11)$$

Where:

ς = 1, 2, …., and m=2^j $with\ j = 0\ and\ 1, 2 \ldots, J,\ \ i = 1,\ 2 \ldots,\ 2m.$

The explicit form of integrals in equation 11 can be written as:

$$P^w_{i,ς}(x) = \{\quad 0, \qquad if\ 0 \leq x < \vartheta_1(i) \qquad \frac{(x-\vartheta_1)^ς}{ξ!},$$

To determine the findings of a system of partially SP initial (first order) and boundary value (second order) problems by the HWM, the following integrals are used as:

$$P^{w}_{i,\varsigma}(x) = \int_0^x h_i^w(t)dt.$$

(13)

The function of Haar wavelet complies with the following characteristic.:

$$P^{w}_{i,\varsigma}(x) = \{ (x - \sigma_0), (\sigma_2 - x), \quad 0, \quad if \quad \delta_0 \leq x < \delta_1 \quad if \quad \delta_1 \leq x < \delta_2 \; elsewhere$$

(14)

$$P^{w}_{i,\varsigma+1}(x) = \int_0^x P^{w}_{i,\varsigma}(x)dt, \quad \varsigma = 1, 2, \ldots \tag{15}$$

and

$$C^{w}_{i,\varsigma}(x) = \int_0^1 P^{w}_{i,\varsigma}(x)dt, \quad \varsigma = 1, 2, \ldots \tag{16}$$

For $\varsigma = 2$, $P^{w}_{i,\varsigma}(x)$ contains the following functions:

$$P^{w}_{i,2}(x) = \{ \quad 0, \qquad if \quad 0 \leq x < \vartheta_1(i) \qquad \frac{(x-\vartheta_1)^{\varsigma}}{2!}, \quad if \; \vartheta_1(i)$$

(17)

The fact that Haar functions constitute an orthogonal basis, i.e.,

$$\int_0^1 h_i^w(x) h_{\tilde{\imath}}^w dt = \delta_{i,\tilde{\imath}}, \tag{18}$$

Where $\delta_{i,\tilde{\imath}}$ represents the Kronecker delta which Mallet describes in reference Mallet (1989) in detail. Additionally, any randomly chosen twice f(x) on [0,1] is an integrable function that has been conceivably approximated as piece-wise constant function in each sub-interval.

$$\sum_{i=1}^{\infty} a_i h_{\tilde{\imath}}^w = f(x) \tag{19}$$

The series comes to an end at 2M terms to approximate the solution. The coefficients a_i of Haar wavelet are assessed as:

$$a_i =< h^w(x), y(x) > \quad = \int_0^1 y(x).\overline{h^w(x)}dx.$$

(20)

3 Construction of Haar Wavelet in Uniform Manner

This section describes the study for finding the approximation of solution of linear initial value problem system with partial singular perturbation.

3.1 Scheme for Initial Value Problem with first-Order Partially Singular Perturbation

$$\varepsilon u_1'(x) + \alpha_0 u_1(x) + \alpha_1 u_2(x) = r_1(x), \tag{21}$$

$$u_2'(x) + \alpha_2 u_1(x) + \alpha_3 u_2(x) = r_2(x), \ x \in (0, 1], \tag{22}$$

With initial conditions

$$u_1(0) = a_1, \ u_2(0) = a_2, \tag{23}$$

Presume that in order to solve the above system,

$$u_1'(x) = \sum_{i=1}^{2N} [q_i^1 H_i^W(x)], \tag{24}$$

and,

$$u_2'(x) = \sum_{i=1}^{2N} [q_i^2 H_i^W(x)], \tag{25}$$

Following results of the Haar solution for system of partially SPIVP are obtained using integration equation (24) and (25):

$$u_1(x) = \sum_{i=1}^{2N} [q_i^1 P_i^W(x)) + u_1(0)], \tag{26}$$

$$u_2(x) = \sum_{i=1}^{2N} [q_i^2 Q_i^W(x)) + u_2(0)], \tag{27}$$

Taking the value of $u_1(x), u_1'(x), u_2(x)$, and $u_2'(x)$ from equation (24)-(27) and plugging them into equation (21) and (22), the system of equations is as follows:

$$\sum_{i=1}^{2N} q_i^1(\varepsilon H_i^W(x) + \alpha_0(x)\, P_i^W(x)) + \alpha_1(x) \sum_{i=1}^{2N} q_i^2(P_i^W(x)) = r_1(x)-$$

$$\alpha_0(x)u_1(0) - \alpha_1(x)u_2(0) \; \forall x \in [0,1]. \quad (28)$$

and,

$$\sum_{i=1}^{2N} q_i^1(\varepsilon H_i^W(x) + \alpha_0(x)\, P_i^W(x)) + \alpha_1(x) \sum_{i=1}^{2N} q_i^1(P_i^W(x)) = r_2(x)-$$

$$\alpha_2(x)u_1(0) - \alpha_3(x)u_2(0) \; \forall x \in (0,1]. \quad (29)$$

The equations (28) and (29) are linear equations with uniform Haar wavelet coefficients q_i^1 and q_i^2 that are unknown and solved using the gauss elimination method. The uniform Haar wavelet coefficients values q_i^1 and q_i^2 is accordingly inserted in equations (26) and (27), which is uniform Haar approximate solution of the system of first-order linear partially SPIVPs.

3.2 Scheme for Finding the Approximate Solution of Second-Order Partially Singularly Perturbed Boundary Value Problem

$$-\varepsilon u_1''(x) + \alpha_0 u_1(x) + \alpha_1 u_2(x) = r_1(x), \quad (30)$$

$$u_2''(x) + \alpha_2 u_1(x) + \alpha_3 u_2(x) = r_2(x), \; \forall x \in (0, 1], \quad (31)$$

with respect to boundary conditions:

$$u_1(0) = a_1, \; u_2(0) = a_2, \; u_1(1) = a_3, \; u_2(1) = a_4, \quad (32)$$

For this system, consider

$$u_1'(x) = \sum_{i=1}^{2N} [q_i^1 H_i^W(x)], \quad (33)$$

$$u_2''(x) = \sum_{i=1}^{2N} [q_i^2 H_i^W(x)], \quad (34)$$

Integrating (33) from 0 to x gives us

$$u_1'(x) = \sum_{i=1}^{2N} [q_i^1 P_i^W(x)) + u_1(0)], \quad (35)$$

In the same way integrating equation (34)

$$u_2'(x) = \sum_{i=1}^{2N} [q_i^2 Q_i^W(x)) + u_2(0)], \quad (36)$$

Equations (37) and (38) are obtained when integrate equations (35) and (36) from 0 to x, respectively

$$u_1(x) = \sum_{i=1}^{2N} (q_i^1 Q_i^W(x)) + xu_1'(0) + u_1(0), \quad (37)$$

And,

$$u_2(x) = \sum_{i=1}^{2N} (q_i^2 Q_i^W(x)) + xu_2'(0) + u_2(0), \quad (38)$$

In addition, by integrating equations (33) and (34) from 0 to 1, $u_1'(0)$ and $u_2'(0)$ are shown below:

$$u_1'(0) = u_1(1) - u_1(0) - \sum_{i=1}^{2N} q_i^1 * O_i(x), \quad (39)$$

And,

$$u_2'(0) = u_2(1) - u_2(0) - \sum_{i=1}^{2N} q_i^2 * O_i(x), \quad (40)$$

Here,

$$O(x) = \int_0^1 P(x)dx. \quad (41)$$

By substituting $u_1'(0)$, and $u_2'(0)$ values from equations (39) and (40) into equations (37) and (38), then the Haar solutions of partially SPBVPs are as follows:

$$u_1(x) = \sum_{i=1}^{2N} q_i^1 (Q_i^W(x)) + x(u_1(0) - u_1(1) + \sum_{i=1}^{2N} q_i^1 O_i(x)) + u_1(0), \quad (42)$$

$$u_2(x) = \sum_{i=1}^{2N} q_i^2(Q_i^W(x)) - x(u_2(0) - u_2(1) + \sum_{i=1}^{2N} q_i^2 O_i(x)) + u_2(0), \quad (43)$$

By inserting the expressions of $u_1(x)$ and $u_2(x)$, $u_1'(x)$ *and* $u_2'(x)$from equations (33), (34), (42) and (43) in equations (30) and (31), the following system of linear equations as shown below:

$$\sum_{i=1}^{2N} q_i^1(-\varepsilon H_i^W(x) + \alpha_0(x)(Q_i(x) - xO_i(x)) + \sum_{i=1}^{2N} q_i^2 \alpha_1(x)((Q_i(x) - xO_i(x)) = r_1(x) - \alpha_0(x)(x(-u_1(0) + u_1(1)) + u_1(0)) - \alpha_1(x)(x(u_2(1) - u_2(0)) - u_2(0)), \quad (44)$$

and,

$$\sum_{i=1}^{2N} q_i^2(H_i^W(x)) + \alpha_3(x)(Q_i(x) - xO_i(x)) + \sum_{i=1}^{2N} q_i^1 \alpha_2(x)((Q_i(x) - xO_i(x)) = r_2(x) - \alpha_2(x)(x(-u_1(0) + u_1(1)) + u_1(0)) - \alpha_3(x)(x(-u_2(0) + u_2(1)) \quad . (45)$$

The system of linear equations that are represented in equations (44) and (45) has uniform Haar wavelet coefficients q_i^1 and q_i^2. Moreover, any approach accessible in the literature can be used to find the unknowns, such as using the Gauss elimination method (row reduction algorithm). On substitution of these unknown q_i^1 in equation (42) and q_i^2 in equation (43) to locate the second-order linear partially SPBVP system's uniform Haar wavelet approximation.

4 Creation of Non-Uniform Meshes

A piece-wise mesh is a Shishkin mesh (multidimensional variant of a tensor-product mesh). The selection of the referred to as transition parameter(s), or the location(s), where the mesh size drastically alters, is what sets a Shishkin mesh is distinct from other piecewise meshes. Shishkin (1988). Term "Shishkin mesh" is one that many numerical analysts have heard of, however, Some of them might not completely comprehend how the choice of transition parameter(s), and therefore, the mechanism of this mesh, delivers accuracy regardless of how little the solitary perturbation parameter is. Shishkin mesh, which is refined inside layers, is added in order to

resolve the layer in the solution of given problem. The strength and position of the layers serve as the foundation for this mesh. For a thorough description of its qualities, see (Roos et al., 2008).

4.1 Grid Structure

The following are the several types of non-uniform meshes used in this study for which the Haar wavelet approach is applied:

Mesh I Generate a non-uniform mesh see Lepik (2014), $\varsigma_x^{N_x}$ in x-direction and similarly create the mesh $\varsigma_y^{N_y}$ in y-direction with N_x=2M and N_y=2M respectively, total number of x and y directional points.

Mesh I generation algorithm The piece-wise uniform and non-uniform fitting mesh/grids are discussed here:

The definition of the p-mesh, or non-uniform grid is:

$$\overline{x_j} = \frac{1-p^i}{1-p^M},\ \text{j=0,1,2….M,}$$

$$\text{x(j)} = \frac{-\bar{x}(j)-\bar{x}(j-1)}{p^M-1},\ \text{j=1,2….M,}$$

Mesh II (Shishkin Mesh) Create the Shishkin mesh, also known as the x-direction, which is likewise, create the mesh $\varsigma_x^{N_x}$, and likewise, create the mesh, $\varsigma_y^{N_y}$ in direction of y, with N_x=2M and N_y=2N respectively, total number of x and y directional points.

4.2 Algorithm for Generation Mesh II

• Configure the transitional parameter ρ_x as $\rho_x = min\{\frac{1}{4}, k_x \varepsilon \log log\, M_x\}$, where k_x based on the coefficient of the response term.

• Create three subintervals from the interval [0, 1] as $[0, \rho_x]$, $[\rho_x, 1-\rho_x]$ and $[1-\rho_x, 1]$.

• Locate $\frac{M_x}{4}$ mesh points within every sub-interval $[0, \rho_x]$ and $[1-\rho_x, 1]$ the mesh spacing is such that $\Delta\bar{t}_i$ contain in these subintervals $\frac{4\rho_x}{N_x}$. Put $\frac{N_x}{2}$ points in $[\rho_x, 1-\rho_x]$. As a result, the mesh distance $\Delta\bar{t}_i$ in this interval is $\frac{2(1-2\rho_x)}{M_x}$.

• Consider the mesh point to be

$$\Delta\bar{t}_i = \{ i\Delta\bar{t}_i,\ \rho_t + \left(i - \frac{M_t}{4}\right)\Delta\bar{t}_i,\quad 1-\rho_x + \left(i - \frac{3M_x}{4}\right)\Delta\bar{t}_i,\quad i = 0, 1, .., \frac{N_x}{4},$$

$$i = \frac{M_x}{4} + 1, ..., \frac{3M_x}{4},\quad i = \frac{3M_x}{4} \qquad (46)$$

To obtain the mesh $\varsigma_x^{N_x} = \{\bar{t}_i\}_0^1$.

• Finally, define the collocation points as follows using these grid points: $\frac{\dot{x}_{i-1}+\dot{x}_i}{2}$, i=1, 2,...$N_x$.

5 Convergence and Uniform Haar Wavelet Scheme Error Analysis

The 2D Haar wavelet technique's convergence analysis is in the L^2-norm. As upper bound of integral $p_{i,1}(x)$ is higher than the lower bound, conclude that the convergence theorem must be derived from the bound.

Theorem 1 Consider the integral of the Haar function $h_i^W(x)$ as described in (11) and (16) respectively as $P^w_{i,1}(x)$ and $P^w_{i,2}(x)$, based on the range [0, 1]. The upper limits for these integrals are therefore provided as follows:

$$h_i^W(x) \leq 1,\ P^w_{i,2}(x) \leq K\left(\frac{1}{2^j+1}\right)^2,\ i > 1,\ P^w_{i,1}(x) \leq \frac{1}{2^j+1},\ with\ i > 1, \text{ and } K = \frac{8}{\lfloor(\varsigma+1/2\rfloor!)^2}.$$

Proof: For the proof of Theorem 1, authors refer Wichailukkana et al., (2016) and Deswal et al., (2022).

Definition 1. The L^2-norm of the approximation at the highest degree of resolution J is given by: $||e_J^r(x, y)||_2 = \{\int\int_D e_J^r(x, y)^2 dx\, dy\}^{\frac{1}{2}}$. Here, (x, y) is in D and D is the rectangular domain that is said to be the L^2-norm of the average error.

Theorem 2 Assume that y′ and y″ are real and enclosed by [a, b]. Whenever J = 0, 1, or 2 for any M = 2^J, and α = 0, 1, 2, 3....P, where P is the positive number, y be the exact solution and Y_M^{α} is the Haar solution and then:

$$||Y_M^{\alpha} - y|| \text{ on } L_{\infty}(a, b) \leq O\left(\frac{1}{M^2}\right), \quad J \to \infty, \quad and \quad P \to \infty.$$

(47)

L_{∞}(a, b) be the interval (a, b)'s infinity norm.

Proof: For the proof of the Theorem 2, see (Deswal et al., (2022) and Liu at al., (2022)).

Theorem 3 Haar integral $P^w_{\alpha,i}(x)$ in (11) and (15) on [0, 1] are defined. Then the maximum possible upper bound of $P^w_{\alpha,i}(x)$ is as below:

$$P^w_{\alpha,1}(x) \leq 1,\ P^w_{0,i}(x) \leq 1/2,\ P^w_{\alpha,i} \leq 1/\alpha!\ ,\ P^w_{1,i}(x) \leq \frac{1}{2^j+1} \text{ if } i>1,$$

Where $C(\alpha) = \frac{8}{(3(\lfloor(\alpha+1)/2\rfloor)}$.

Proof: For the detailed proof of the Theorem 3, see Wichailukkana at al., (2016).

Assumption 1. For the sake of this study, assume that $\varepsilon \leq \frac{1}{N}$.

Theorem 4 Wichailukkana at al., (2016). If assumption 1 is accurate, Shishkin mesh with $\sigma \geq k + 1$, there is $||y - y_{App}^N|| \leq C\frac{1}{N^k}(ln\, N)^k)$, where, y is an exact solution of problem and y_{App}^N represents the approximate solution.

Proof: The triangle inequality and Lemma 1 easily lead to the conclusion.

Lemma 1: If presumption 1 is correct, the results for Shishkin mesh are as follows.

Algorithm for numerical study of partially singularly perturbed problems via Uniform Haar Wavelet Method

Consider J∈ N,

Step I. Compute the uniform Haar matrix $h_i^W(x)$ from equation (7) as the Haar function is given as below:

$h_i^W(x) = \{\ 1,\ -1,\ 0,\quad if\quad \vartheta_1(i) \leq x < \vartheta_2(i)\ \ if\ \vartheta_2(i) \leq x < \vartheta_3(i)\ elsewhere$

Step II. Compute the $P^W{}_{i,1}(x)$ and $P^W{}_{i,2}(x)$, from equation (11) and equation (16) by creating the Haar wavelet family using the integral as below:

$$P_{i,\varsigma} = \int_A^x \int_A^x \ldots\ldots\ldots \int_A^x h_i^w(t)dt^\varsigma = \frac{1}{\varsigma-1}\int_A^x (x-t)^{\varsigma-1} h_i^w(t)dt,$$

Where:

ς = 1, 2, …., and i = 1, 2…, 2m, m=2^j, $j = 0, 1, 2\ldots, J$.

Step III. Construct the scheme for first-order SPIVPs given by (21)-(29) and construct the scheme for scheme for second order partially SPBVPs given by equation (30) to equation (45).

Step IV. Select the grid points from the grid structure.

Step V. Using the steps III to IV, construct the LHS of linear algebraic expression for the approximate Haar solution of singularly perturbed initial/boundary value problems as below.

$$r_1(x) - \alpha_0(x)u_1(0) - \alpha_1(x)u_2(0) \quad x \in [0,1],$$

and,

$$r_2(x) - \alpha_2(x)u_1(0) - \alpha_3(x)u_2(0) \quad x \in (0,1].$$

Similarly construct the expression

$$r_1(x) - \alpha_0(x)(x(-u_1(0) + u_1(1)) + u_1(0)) - \alpha_1(x)(x(u_2(1) - u_2(0)) - u_2(0)),$$

and,

$$r_2(x) - \alpha_2(x)(x(-u_1(0) + u_1(1)) + u_1(0)) - \alpha_3(x)(x(-u_2(0) + u_2(1)) - u_2(0)).$$

Step VI. To approximation the Haar solutions $u_1$and $u_2$on non-uniform grids, evaluate the linear algebraic system of equations provided in step V.

6 Results and Discussion

To demonstrate the UHWM on various meshes, in this paper, numerical problem of a linear partially singularly perturbed system of initial value problems (first-order) as well as one numerical problem of a partially SPBVP (second-order) has been taken to the study. To show the uniform Haar wavelet method on various meshes, the maximum absolute residual errors with the maximum absolute values are listed and compared to Raza and Khan (2021) and Matthews at al., (2002), the conventional finite difference operator method and the uniform parameter scheme, respectively.

Problem-1 Consider an initial value problem with a partial system of singularly perturbed problem given below:

$$\varepsilon u_1'(x) + (x + 2)u_1(x) - \left(\frac{x}{2} + 1\right)u_2(x) = 5x + \frac{1}{2}, \quad (48)$$

$$u_2'(x) - (x + 1)u_1(x) - (x + 2)u_2(x) = \exp exp\,(x) * x\,, \; x \in (0, 1], \quad (49)$$

with initial conditions:

$$u_1(0) = 2 \text{ and } u_2(0) = 2. \quad (50)$$

Solution: The Uniform Haar Wavelet Method in discretized form is expressed as

$$\varepsilon \sum_{i=1}^{2N} [q_i^1(H_i^W(x))] + (2 + x) \sum_{i=1}^{2N} [q_i^1(P_i^W(x)) + 2] - (1+\tfrac{x}{2})\, q_i^1(P_i^W(x) + 2 = 5x + \tfrac{1}{2} \quad (51)$$

and,

$$\sum_{i=1}^{2N} [q_i^2(H_i^W(x))] - (1 + x)[\sum_{i=1}^{2N} q_i^1(P_i^W(x) + 2] + (2 + x)\,)[\sum_{i=1}^{2N} q_i^2(P_i^W(x) + 2]$$

$$= x * exp(x). \quad (52)$$

After simplifying the system (51) and (53)

$$\varepsilon \sum_{i=1}^{2N} [q_i^1(H_i^W(x))] + 2\sum_{i=1}^{2N} [q_i^1(P_i^W(x))] + x\sum_{i=1}^{2N} [q_i^1(P_i^W(x))] - \sum_{i=1}^{2N} [q_i^2(P_i^W(x))]$$

$$- \frac{x}{2}\sum_{i=1}^{2N} q_i^2\left(P_i^W(x)\right) = 5x + \frac{1}{2}\text{-6-2t}$$

(53)

and,

$$\sum_{i=1}^{2N} [q_i^2(H_i^W(x))] - \sum_{i=1}^{2N} [q_i^1(P_i^W(x))] - 2 - x - x[q_i^1(P_i^W(x))] + 2x + 2\sum_{i=1}^{2N} [q_i^2 P_i^W(x)$$

$$+ 4 + x\sum_{i=1}^{2N} [q_i^2(P_i^W(x))] = x * exp(x).$$

(54)

$$\varepsilon \sum_{i=1}^{2N} [q_i^1(H_i^W(x))] + 2\sum_{i=1}^{2N} [q_i^1(P_i^W(x))] + x\sum_{i=1}^{2N} [q_i^1(P_i^W(x))] - \sum_{i=1}^{2N} [q_i^2(P_i^W(x))] - \frac{x}{2}\sum_{i=1}^{2N} q_i^2\left(P_i^W(x)\right) = 3x + \left(\frac{11}{2}\right),$$

(55)

and,

$$\sum_{i=1}^{2N} [q_i^2(H_i^W(x))] - \sum_{i=1}^{2N} [q_i^1(P_i^W(x))] + 2 + 4x - x\sum_{i=1}^{2N} [q_i^1(P_i^W(x))] + 2\sum_{i=1}^{2N} [q_i^1(P_i^W(x))] + x\sum_{i=1}^{2N} [q_i^2(P_i^W(x))]$$

(56)

The numerical computed results based on UHWM for the partially SPIVP with different meshes and different parameters ε, J are reported in the Tables 1-2 and Table-4. Tables reports the maximum residual error for different non uniform grids which clearly indicates that the present method gives good accuracy as comparison with existing techniques such as non- uniform HWM and finite difference operator method. Figures 1-15 show the numerical solutions for u_1 and u_2 and corresponding maximum absolute residual error in 2- dimensional for the different values of parameters ε, J, M_x, M_y and ϑ_i, i = 1, 2, 3. This shows that the accuracy has been improved with comparison to the other existing schemes. Different level of resolution has been carried out to examine the accuracy of UHWM on different meshes.

Results of maximum absolute residual error for different values of 2N with Shishkin-mesh is shown in Table-3 by non- uniform HWM and recoded the maximum absolute residual error therein are 3.5749e-14 and 6.6391e-14 respectively for 2N= 128 and 2N=256 with $\varepsilon = \frac{1}{2^6}$.The maximum residual error of present algorithm is listed in Table-2 with residual error 2.8649e-15 and 6.0455e-15 for the same collocation point and perturbation parameter. For other values of 2N, a marginal increase in accuracy is shown.

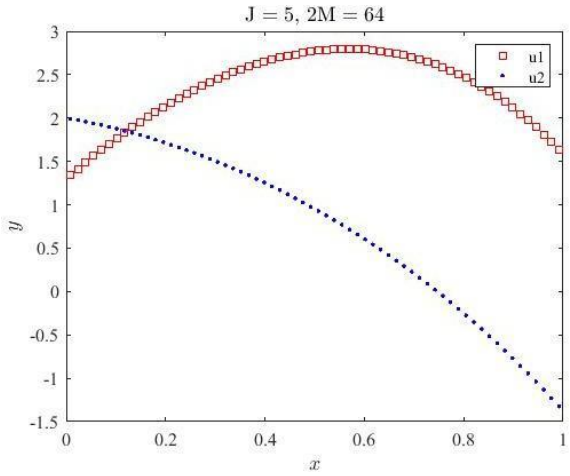

Fig.1: Uniform Haar solution for $\varepsilon = \frac{1}{2^8}$, J=5 on p-mesh.

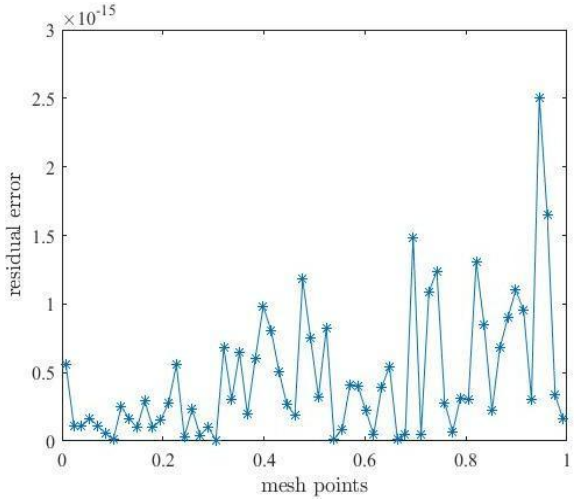

Fig.2: Residual error for $\varepsilon = \frac{1}{2^8}$, J=5 on p-mesh.

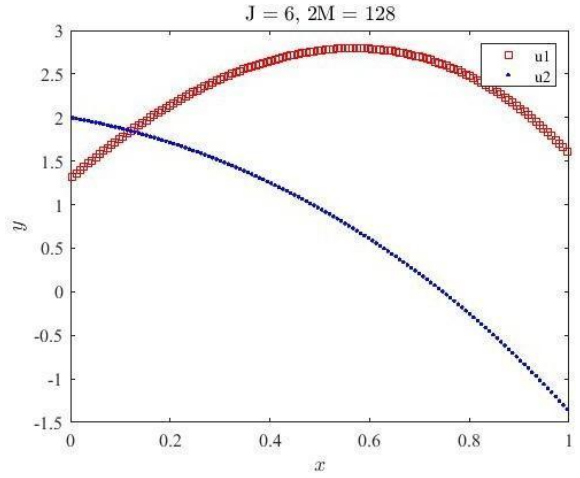

Fig.3: Uniform Haar solution for $\varepsilon = \frac{1}{2^8}$, J=6 on p-mesh.

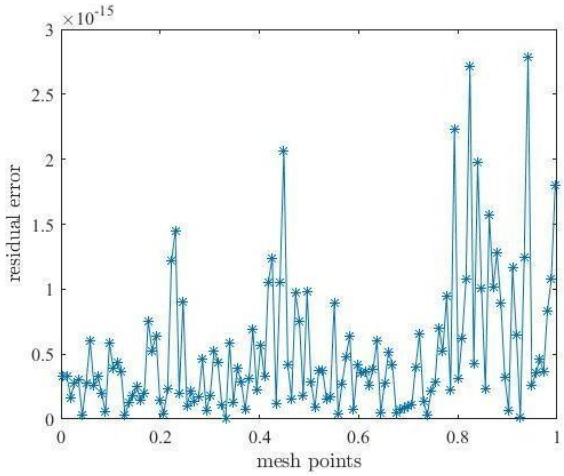

Fig.4: Residual error for $\varepsilon = \frac{1}{2^8}$, J=6 on p-mesh.

Fig.1 illustrates the uniform Haar solution for J=5 and 2M=64 for Problem-1 on p-mesh with $\varepsilon = \frac{1}{2^8}$. By using the numerical technique described in Section 5, the Haar solutions u_1 and u_2 are drawn on various grid points. With mesh points of 2M=64 and a resolution level of J=5, the corresponding maximum absolute residual error is shown in Fig.2. The uniform Haar solutions $u_1$and u_2 are presented in Fig.3 for J=6 and 2M=128 for $\varepsilon = \frac{1}{2^8}$. The uniform Haar solution can be more closely approximated by increasing the mesh points and lowering the value of epsilon. On p-mesh, Fig.4 illustrates the corresponding maximum absolute residual error occurs in the uniform Haar solution for level of resolution J=6, and mesh point 2M=128 with perturbation parameter $\varepsilon = \frac{1}{2^8}$. Fig.2 and Fig.4 make it abundantly evident that the maximum absolute residual error is less when the mesh point is increased in the numerical algorithm of the uniform Haar wavelet approach.

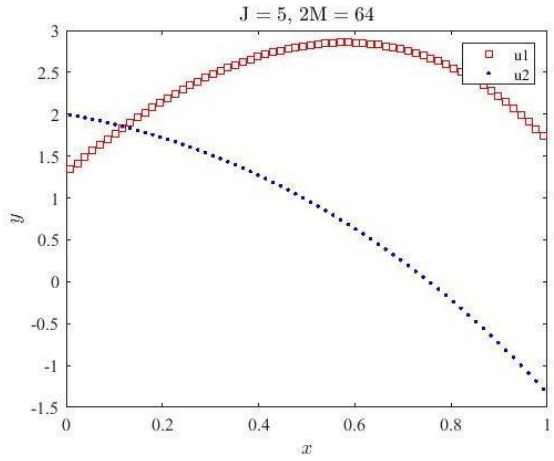

Fig.5: Uniform Haar solution for $\varepsilon = \frac{1}{2^6}$, J=5 on p-mesh.

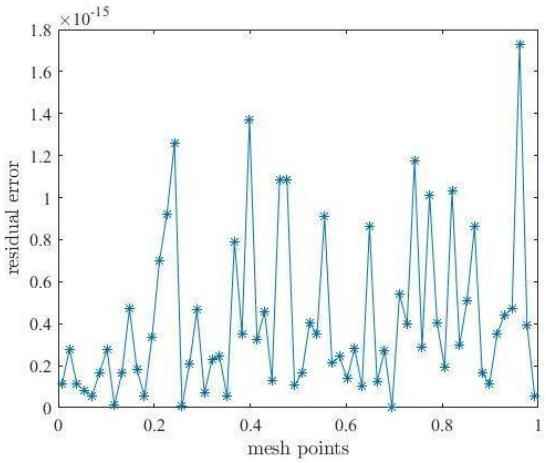

Fig.6: Residual error for $\varepsilon = \frac{1}{2^6}$, J=5 on p-mesh.

p-mesh.

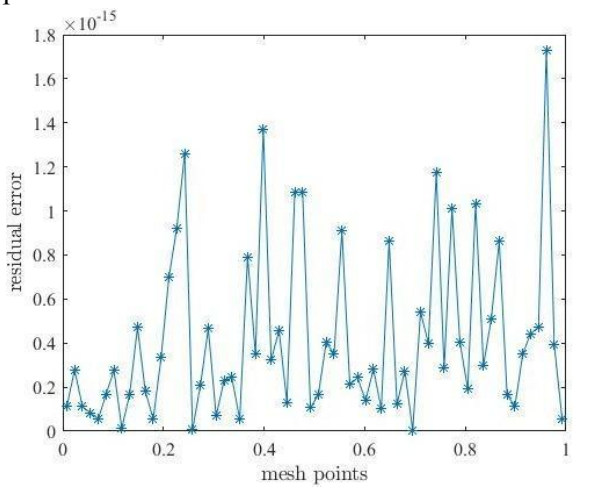

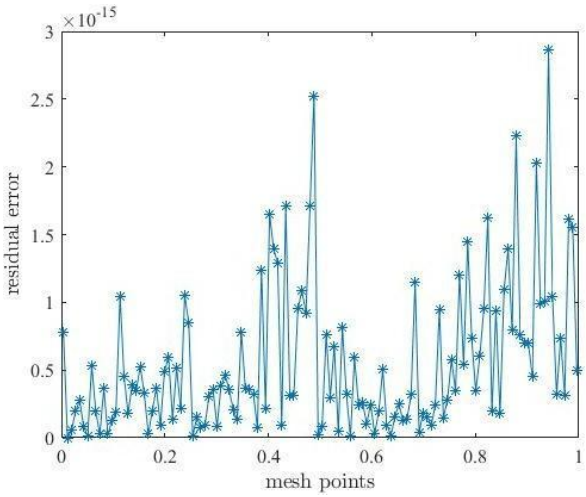

Fig.7: Residual error for $\varepsilon = \frac{1}{2^{10}}$, J=5 on p-mesh.

Fig.8: Residual error for $\varepsilon = \frac{1}{2^{10}}$, J=6 on p-mesh.

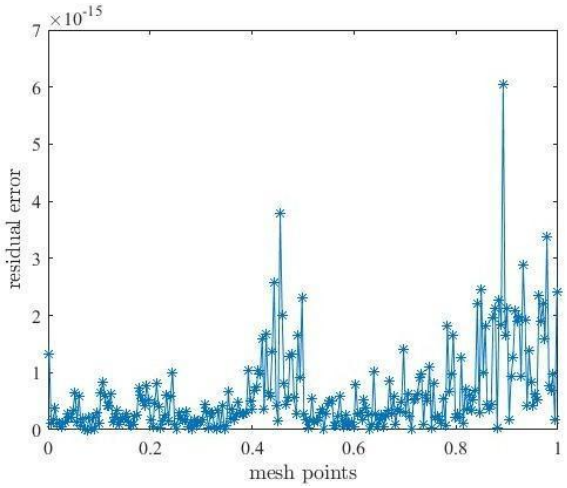

Fig.9: Residual error for $\varepsilon = \frac{1}{2^{10}}$, J=7 on p-mesh.

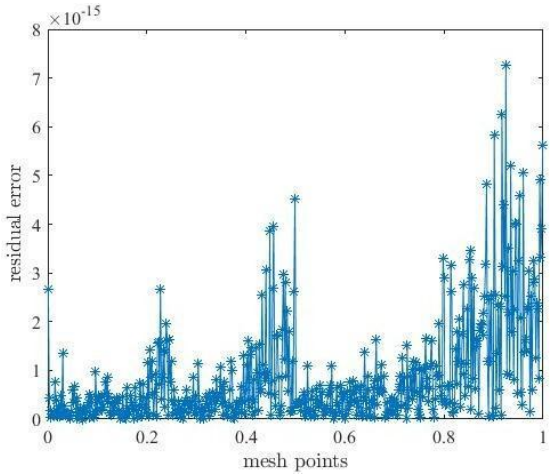

Fig.10: Residual error for $\varepsilon = \frac{1}{2^{10}}$, J=8 on p-mesh.

Fig.5 shows the graph of uniform Haar wavelet solutions u_1 and u_2 for J=5, and 2M=64 on p-mesh with $\varepsilon = \frac{1}{2^6}$. The corresponding residual error on the uniform Haar solution is given in Fig.6 for the same values of mesh points and level of resolution. For $\varepsilon = \frac{1}{2^{10}}$ and J=5, the residual error is given in Fig.7. On increasing the level of resolution from J=5 to J=6 and decreases the value of epsilon from $\varepsilon = \frac{1}{2^6}$ to $\varepsilon = \frac{1}{2^{10}}$, the maximum absolute residual error decreases as it has been shown in Fig.6 and Fig.8. Fig.9 shows the maximum absolute residual error for J=7 and $\varepsilon = \frac{1}{2^{10}}$. The maximum residual error further decreases while increasing the mesh points in the method for $\varepsilon = \frac{1}{2^{10}}$ and J=8 on p-mesh as seen in Fig.10.

For the values of different perturbation parameter, Tables 1, 2, and 4 compare the UHWM's maximum absolute residual errors with various levels of resolution with those calculated by the traditional difference operator scheme and the non-uniform HWM for p-mesh. Additionally, Figures 1-10 provide a graph Haar wavelet solution in uniform manner and corresponding residual error. For $\varepsilon = \frac{1}{2^{10}}$, and J=5,6,7,8 the maximum residual error is 2.1719e−15, 2.8649e−15, 6.0455e−15, 7.2646e−15 respectively.

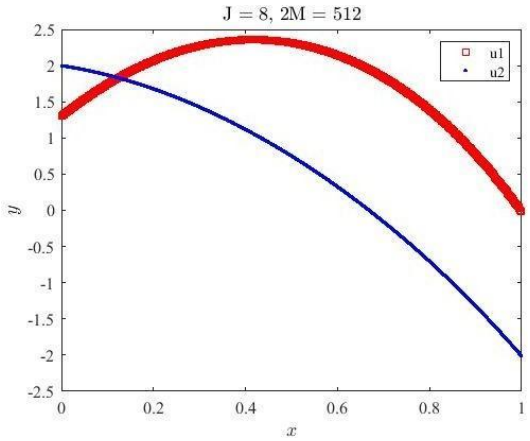

Fig.11: Uniform Haar solution for $\varepsilon = \frac{1}{2^{16}}$, J=8 on Shishkin mesh.

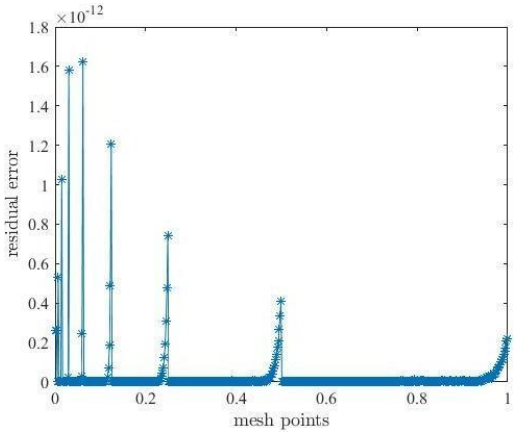

Fig.12: Residual error for $\varepsilon = \frac{1}{2^{16}}$, J=8 on Shishkin mesh.

Fig. 11 and Fig.12 illustrates the uniform Haar solution and the accompanying maximum residual error on the Shishkin mesh caused by calculating the numerical technique described above for level of resolution J=8and $\varepsilon = \frac{1}{2^{16}}$, with residual error $1.6229e^{-12}$. Fig.12 shows that UHWM performs very well on p-mesh then the Shishkin mesh for same values of level of resolution J=8, and perturbation parameter $\varepsilon = \frac{1}{2^{16}}$.

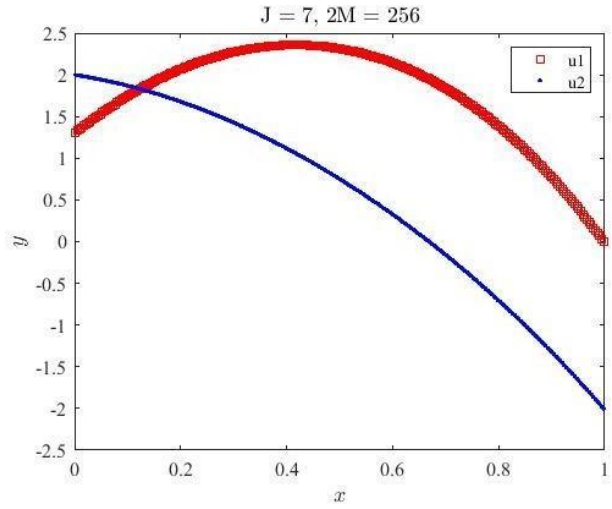

Fig.13: Uniform Haar solution for $\varepsilon = \frac{1}{2^{16}}$, J=7 on Shishkin mesh.

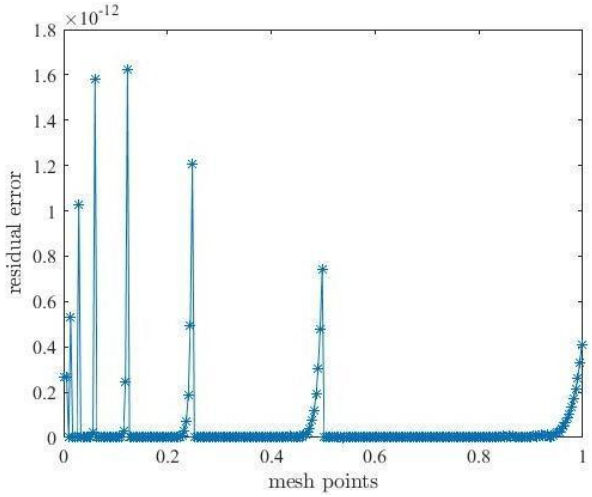

Fig.14: Residual error for $\varepsilon = \frac{1}{2^{16}}$, J=7 on Shishkin mesh.

Fig.13 and Fig.14 illustrates the numerical solution and corresponding maximum absolute residual errors on Shishkin mesh for the perturbation parameter's value $\varepsilon = \frac{1}{2^{16}}$, with level of resolution J=7 which draws the conclusion that on increasing the resolution level or the mesh points in the method the accuracy is improved further.

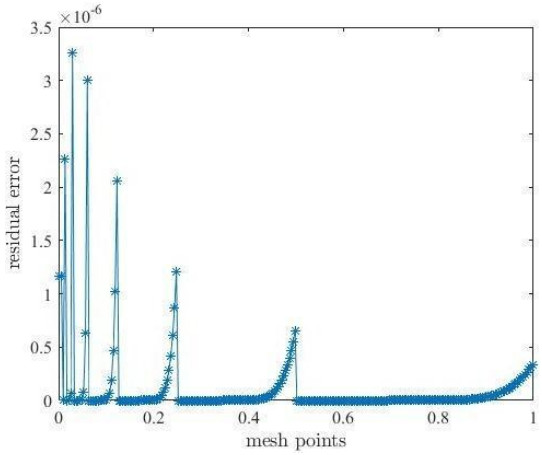

Fig.15: Residual error for $\varepsilon = \frac{1}{2^{34}}$, J=8 on Shishkin-mesh.

On Shishkin mesh, the accompanying maximum absolute residual error with $\varepsilon = \frac{1}{2^{34}}$ and level of resolution J=8 is given in Fig.15. Fig. 15 shows the stability of the UHWM for small values of perturbation parameter ε. For Shishkin mesh with perturbation parameter $\varepsilon = \frac{1}{2^{16}}$ and the level of resolution $J = 7$ the maximum residual error decreased to $1.6229e^{-12}$. For particular case of J=8 and $\varepsilon = \frac{1}{2^{34}}$, the residual error has been $3.2587e^{-6}$.

Table 1: Uniform Haar Wavelet method on p-mesh, the calculation of maximum absolute residual errors for various values of ε.

ε	$J_{64}(x_j)$	$J_{128}(x_j)$	$J_{256}(x_j)$	$J_{512}(x_j)$	$J_{1024}(x_j)$	$J_{2048}(x_j)$
$\frac{1}{2^8}$	2.5041e−15	2.7860e−15	4.4892e−15	8.1365e−15	1.1256e−14	2.7267e−13
$\frac{1}{2^{10}}$	2.1719e−15	2.8649e−15	6.0455e−15	7.2646e−15	1.0853e−14	1.4999e−12
$\frac{1}{2^{12}}$	1.8076e−15	2.7998e−15	5.0810e−15	8.2123e−15	9.4842e−15	1.5477e−12
$\frac{1}{2^{14}}$	2.8649e−15	3.4504e−15	5.2363e−15	7.5731e−15	9.0513e−15	1.5477e−12
$\frac{1}{2^{16}}$	2.8103e−15	2.7270e−15	3.6329e−15	7.3643e−15	4.9925e−12	3.6597e−12
$\frac{1}{2^{18}}$	1.6480e−15	3.8246e−15	4.9273e−15	5.8066e−15	1.0564e−14	7.5797e−12
$\frac{1}{2^{20}}$	4.7011e−15	5.8204e−15	8.6092e−15	1.3666e−14	2.6653e−15	8.2536e−11
$\frac{1}{2^{22}}$	3.2344e−15	3.8242e−15	1.1978e−14	1.0505e−14	2.7449e−11	4.0708e−11
$\frac{1}{2^{24}}$	2.1320e−15	3.7088e−15	5.3087e−15	6.7364e−15	2.8213e−11	4.3110e−11

$\frac{1}{2^{26}}$	1.7842e−15	3.1563e−15	4.7926e−15	6.8136e−15	2.8385e−11	4.4727e−11
$\frac{1}{2^{28}}$	6.1956e−15	5.7645e−15	6.6856e−15	1.5061e−14	2.8827e−11	4.5758e−11
$\frac{1}{2^{30}}$	8.4273e−15	1.0492e−14	1.0320e−14	1.3319e−14	2.8260e−11	4.4787e−11
$\frac{1}{2^{32}}$	1.7764e−15	1.8128e−15	2.3878e−15	2.6320e−14	2.8895e−11	8.1765e−11
$\frac{1}{2^{34}}$	2.2569e−15	2.6819e−15	2.3332e−15	3.5774e−15	2.8591e−11	4.4877e−11
$\frac{1}{2^{36}}$	2.4911e−15	2.7721e−15	2.1862e−15	3.1407e−15	2.8591e−11	4.4827e−11
$\frac{1}{2^{38}}$	1.9221e−15	2.6073e−15	3.2032e−15	3.6655e−15	2.8871e−11	4.5883e−11
$\frac{1}{2^{40}}$	2.3107e−15	2.2794e−15	2.5162e−15	4.5042e−15	2.8853e−11	4.7851e−11

Table 2: Uniform Haar Wavelet method on Shishkin-mesh, the calculation of maximum absolute residual errors for various values of ε.

ε	$J_{32}(x_j)$	$J_{64}(x_j)$	$J_{128}(x_j)$	$J_{256}(x_j)$	$J_{512}(x_j)$	$J_{1024}(x_j)$
$\frac{1}{2^{2}}$	9.5063e−16	1.7850e−15	3.8385e−15	4.7998e−15	9.3260e−15	1.0837e−14
$\frac{1}{2^{4}}$	8.9165e−16	2.5041e−15	2.7860e−15	4.4892e−15	8.1365e−15	1.1256e−14
$\frac{1}{2^{6}}$	1.7555−15	2.1719e−15	2.8649e−15	6.0455e−15	7.2646e−15	1.0853e−13
$\frac{1}{2^{8}}$	2.5828e−14	2.3849e−14	2.9345e−14	2.7714e−14	2.3627e−14	2.3657e−14
$\frac{1}{2^{10}}$	6.4320e−14	6.5475e−14	6.1132e−14	6.4143e−14	6.3099e−14	6.4824e−14
$\frac{1}{2^{12}}$	3.5034e−13	3.5781e−13	3.5680e−13	3.5675e−13	3.5829e−13	3.5792e−13
$\frac{1}{2^{14}}$	7.6351e−13	7.7651e−13	7.7847e−13	7.8022e−13	7.7947e−13	1.5477e−12
$\frac{1}{2^{16}}$	1.5921e−12	1.6133e−12	1.6234e−12	1.6234e−12	1.6229e−12	1.6259e−12
$\frac{1}{2^{18}}$	3.1812e−12	3.2284e−12	3.2437e−12	3.2484e−12	3.2485e−12	7.5797e−12
$\frac{1}{2^{20}}$	6.1287e−12	6.2209e−12	6.2516e−12	6.2595e−12	6.2592e−12	6.2552e−12
$\frac{1}{2^{22}}$	4.3606e−10	4.4327e−10	4.4557e−10	4.4557e−10	4.4568e−10	4.4571e−10
$\frac{1}{2^{24}}$	6.7552e−10	6.8665e−10	6.8949e−10	6.9020e−10	6.9038e−10	6.9042e−10
$\frac{1}{2^{26}}$	1.8065e−08	1.8348e−08	1.8419e−08	1.8442e−08	1.8443e−08	4.4727e−11
$\frac{1}{2^{28}}$	1. 8706e−07	1.8820e−07	1.8849e−07	1.8856e−07	1.8858e−07	4.5727e−11
$\frac{1}{2^{30}}$	1.5672e−07	1.5769e−07	1.5793e−07	1.5799e−07	1.5800e−07	4.4787e−11

$\frac{1}{2^{32}}$	1.9171e−06	1.9290−06	1.9320e−06	1.9327e−06	1.9329e−06	1.9330e−06
$\frac{1}{2^{34}}$	3.2325e−06	3.2522e−06	3.2571e−06	3.2583e−06	3.2587e−06	3.2587e−06
$\frac{1}{2^{36}}$	5.2326e−06	5.2638e−06	5.2716e−06	5.2736e−06	5.2741e−06	4.4827e−11

Table 3: Table of the absolute error calculated by non-uniform HWM (Raza and Khan (2021)) at various resolution levels and for various perturbation parameters ϵ for Problem 1 on Shishkin mesh.

ε	$J_{64}(x_j)$	$J_{128}(x_j)$	$J_{256}(x_j)$	$J_{512}(x_j)$	$J_{1024}(x_j)$	$J_{2048}(x_j)$
$\frac{1}{2^{2}}$	2.153e−14	6.661e−15	1.509e−14	1.620e−14	1.509e−14	3.685e−14
$\frac{1}{2^{4}}$	2.087e−14	4.440e−15	1.909e−14	1.554e−14	5.040e−14	7.593e−14
$\frac{1}{2^{6}}$	2.198e−14	3.574e−14	6.639e−14	2.531e−14	9.126e−14	5.890e−13
$\frac{1}{2^{8}}$	9.592e−14	2.349e−13	1.430e−13	2.504e−13	2.802e−13	1.068e−12
$\frac{1}{2^{10}}$	4.447e−13	5.875e−13	3.237e−13	8.477e−13	1.095e−12	5.885e−12
$\frac{1}{2^{12}}$	6.747e−13	1.802e−12	3.347e−12	4.218e−12	5.893e−12	1.138e−11
$\frac{1}{2^{14}}$	5.481e−12	8.047e−13	7.956e−12	2.048e−11	3.311e−11	7.304e−11
$\frac{1}{2^{16}}$	5.390e−11	1.591e−11	1.599e−11	8.026e−11	3.311e−11	7.304e−11
$\frac{1}{2^{18}}$	1.153e−10	6.964e−11	1.599e−11	8.026e−11	3.311e−11	7.304e−11
$\frac{1}{2^{20}}$	6.172e−10	7.896e−10	7.781e−10	2.867e−09	1.194e−09	2.214e−09
$\frac{1}{2^{22}}$	1.286e−09	2.692e−09	4.159e−09	2.429e−09	5.760e−09	1.098e−08
$\frac{1}{2^{24}}$	5.708e−09	1.377e−08	8.824e−09	1.012e−08	2.939e−08	3.297e−08
$\frac{1}{2^{26}}$	4.6880e−08	1.9145e−08	6.1711e−08	9.7442e−08	9.8635e−08	1.0465e−07
$\frac{1}{2^{28}}$	9.8958e−08	1.0455e−07	1.3310e−07	1.5702e−07	3.4662e−07	1.0747e−06
$\frac{1}{2^{30}}$	1.8406e−07	4.8247e−07	3.5228e−07	1.6018e−06	1.9999e−06	3.4653e−06
$\frac{1}{2^{32}}$	2.2135e−06	1.9222e−13	1.089e−12	1.2280e−11	2.8895e−11	8.1765e−11
$\frac{1}{2^{34}}$	1.7542e−14	1.8163e−13	1.0154e−12	1.2091e−11	2.8591e−11	8.4877e−11
$\frac{1}{2^{36}}$	1.9096e−14	1.8829e−13	1.0154e−12	1.2091e−11	2.8591e−11	4.4827e−11
$\frac{1}{2^{38}}$	1.7764e−14	1.8097e−13	1.2020e−12	1.2412e−11	2.8871e−11	4.5883e−11
$\frac{1}{2^{40}}$	3.8636e−14	1.4766e−13	1.1727e−12	1.2459e−11	2.8853e−11	4.4534e−11

Table-1 and Table-2 shows for Problem 1 using the uniform Haar wavelet approach on p-mesh and Shishkin mesh, the maximum residual errors for various perturbation parameters (ε) and levels of resolution (J). Tables 1 and 2 clearly show that the uniform Haar wavelet approach gives a superior approximation than the Shishkin mesh for a different value of ε and J by comparing the produced maximal residual errors for various p-meshes. Also, Table-3 shows the maximum residual error on p-mesh by non-uniform HWM. Table-2, Table-3 reflects that, for the value of perturbation parameter $\varepsilon = 2^{-16}, 2^{-20}$ and same level of resolution, the uniform Haar wavelet approach performs better on Shishkin mesh than the non-uniform HWM. The authors draw the conclusion that the non-uniform Haar wavelet approach is ineffective for the SPIVP for Problem 1. This problem has been resolved for small values of ε (highly perturbed problems) on p-mesh and Shishkin mesh using the uniform Haar wavelet approach based on the provided numerical methodology. Tables 2 and 3 show that the numerical methodology of the uniform Haar wavelet approach produces a smaller maximum residual error than the non-uniform HWM. For $\varepsilon = 2^{-16}$ and 2N=64, the maximum residual error jump to 1.5921^{-12} by the UHWM and 5.3906^{-11} by the non-uniform HWM on Shishkin mesh. This reflects the better efficiency of the proposed scheme.

Table 4: Table of Maximum absolute residual errors on the Shishkin-mesh for different values ε calculated by the uniform Haar Wavelet technique.

ε	$J_{32}(x_j)$	$J_{64}(x_j)$	$J_{128}(x_j)$	$J_{256}(x_j)$	$J_{512}(x_j)$	$J_{1024}(x_j)$
10^{-3}	6.4320e-14	6.5475e-14	6.1132e-14	6.3099e-14	6.4823e-14	1.3487e-12
10^{-5}	1.2422e-11	1.1596-13	1.1643e-11	1.1660e-11	1.1663e-11	1.1662e-11
10^{-7}	3.3175e-9	3.3711e-9	3.3849e-9	3.3883e-9	3.3891e-9	3.3894e-9

Table- 4 shows the maximum absolute residual errors on Shishkin mesh for perturbation parameter $\varepsilon = 10^{-3}, 10^{-5}, 10^{-7}$ obtained by UHWM. Table-4 draws a conclusion that, on

increasing the values of perturbation parameters, the maximum absolute residual errors decrease for same number of grid points. Further, Table-4 shows the stability of the present scheme for the values of small perturbation parameter (ε). The uniform Haar wavelet method's precision has been tested using a variety of mesh locations.

Table 5: Table of Maximum absolute residual errors on the Shishkin-mesh for different values ε calculated by the non-uniform Haar Wavelet technique.

ε	$J_{32}(x_j)$	$J_{64}(x_j)$	$J_{128}(x_j)$	$J_{256}(x_j)$	$J_{512}(x_j)$	$J_{1024}(x_j)$
10^{-3}	2.240e-13	4.509e-13	7.458e-13	1.164e-13	3.262e-13	3.921e-12
10^{-5}	2.794e-11	3.088-11	2.548e-11	1.085e-10	3.765e-11	5.273e-11
10^{-7}	1.002e-08	3.236e-09	4.537e-09	5.118e-09	1.468e-08	5.084e-08

Maximum absolute residual errors obtained by the non-uniform HWM on Shishkin Mesh for $\varepsilon = 10^{-3}, 10^{-5}, 10^{-7}$ is given in Table-5 with different mesh points. Table-4 presents better accuracy in Maximum absolute residual errors for same values of perturbation parameter ε and level of resolution (J). The accuracy of UHWM gets improved by compare the Table-4 and Table-5.

Table 6: Table of Maximum absolute residual errors on the Shishkin-mesh for different values of ε calculated by the conventional finite difference operator scheme.

ε	$J_{32}(x_j)$	$J_{64}(x_j)$	$J_{128}(x_j)$	$J_{256}(x_j)$	$J_{512}(x_j)$	$J_{1024}(x_j)$
10^{-3}	3.400e-02	1.810e-02	1.117e-02	7.180e-02	4.270e-03	1.370e-02
10^{-5}	3.400e-02	1.810e-02	1.117e-02	7.180e-02	4.270e-03	1.370e-02
10^{-7}	3.400e-02	1.810e-02	1.117e-02	7.180e-02	4.270e-03	1.370e-02

Table-6 presents the maximum absolute residual errors obtained by the finite difference operator method for different values of ε on Shishkin mesh. The maximum absolute residual error is evaluated on $\varepsilon = 10^{-3}, 10^{-5}, 10^{-7}$ respectively on different grid points. On compare the Table-4

with Table-5 and Table-6, the uniform Haar wavelet yields improved results in comparison to the existing method such as non-uniform HWM and finite difference method.

As a result of its superior interpolation capabilities, the UHWM has been used to this instability problem. For various perturbation parameters and resolution levels, the Haar wavelet technique produces a fast-convergent solution. When the translation parameter is increased over a certain point, the current methods lose their ability to maintain the convergence order. With more points contributing, the precision of the current system is also more effective. As shown in Table-4, the uniform Haar wavelet approach is used to solve this problem for various 2N on Shishkin mesh values. In contrast to the non-uniform HWM and finite difference operator technique, the results based on the uniform Haar wavelet-based methodology give stable and convergent solutions.

Problem-2 The singularly perturbed boundary value problem (second order) is given below as follows:

$$-\varepsilon u''_1(x) + 2(x+1)^2 u_1(x) - (x^3+1)u_2(x) = 2 * exp(x) \quad (57)$$

$$u''_2(x) - 2\cos cos\left(\frac{\pi x}{4}\right)u_1(x) + 2 * 2e^{(1-x)}u_2(x) = 10x + 1 \text{ } x\in(0,1], \quad (58)$$

with the boundary conditions:

$$u_1(0) = 0, u_1(1) = 0,\ u_2(0) = 0, u_2(1) = 0. \quad (59)$$

Solution: The Uniform Haar wavelet Method in its discretized version on problem 2 is expressed as:

$$-\varepsilon \sum_{i=1}^{2N}[q_i^1(H_i^W(x))] + 2(x+1)^2 * \sum_{i=1}^{2N}[q_i^1(Q_i^W(x))] + xu_1'(0)] -$$

$$,(x^3+1)[\sum_{i=1}^{2N} q_i^2(Q_i^W(x)) + xu_2'(0)] =$$

and,

$$\sum_{i=1}^{2N}[q_i^2(H_i^W(x))] - 2 * \cos cos\left(\frac{\pi x}{4}\right) + [\sum_{i=1}^{2N}[q_i^1\left(Q_i^W(x)\right) + xu_1'(0) + u_1(0)] + 2*2\exp(1\text{-}x)$$

$$[\sum_{i=1}^{2N} q_i^2 * (Q_i^W(x)) + xu_2'(0) + u_2(0)] = 10x+1, \quad (59)$$

Simplifying the system of equation (58) and (59),

-

$$\varepsilon \sum_{i=1}^{2N} [q_i^1(H_i^W(x))] + 2(x+1)^2 * \sum_{i=1}^{2N} [q_i^1(Q_i^W(x))] + 2(x+1)^2 * [xu_1'(0)] - (x^3+1) * [xu_2'(0)] = 2 * exp(x)$$

, (60)

and,

$$\sum_{i=1}^{2N} [q_i^2(H_i^W(x))] - 2 * \cos cos\left(\frac{\pi x}{4}\right) + [\sum_{i=1}^{2N} [q_i^1\left(Q_i^W(x)\right) + x \sum_{i=1}^{2N} [-q_i^2 * O_i(x)] +$$

$$2*2\exp(1-x) \quad [\sum_{i=1}^{2N} q_i^2 \quad * (Q_i^W(x)) + x * \sum_{i=1}^{2N} [-q_i^2 * O_i(x)] = 10x+1$$

(61)

Equation (60) and equation (61) are simplified to produce the linear system of equation (62)-(63),

$$-\varepsilon \sum_{i=1}^{2N} [q_i^1(H_i^W(x))] + 2(x+1)^2 * \sum_{i=1}^{2N} [q_i^1(Q_i^W(x))] + 2(x+1)^2 * [x * (-q_i^1(O_i^W(x)))]$$

$$- (x^3+1) * [q_i^2(Q_i^W(x))] - (x^3+1) * [x(-q_i^2(Q_i^W(x))] = 2 * \exp exp(x),$$

(62)

and,

$$\sum_{i=1}^{2N} [q_i^2(H_i^W(x))] - 2 * \cos cos\left(\frac{\pi x}{4}\right) + \sum_{i=1}^{2N} [q_i^1(Q_i^W(x))] - 2 * \cos cos\left(\frac{\pi x}{4}\right) *$$

$$x \sum_{i=1}^{2N} - q_i^2(O_i^W(x)) + 2 * 2$$

(63)

and, the piecewise uniform and non-uniform fitting mesh/grids are the Shishkin -mesh, or non-uniform grid, is:

$$\overline{x}_j = \frac{1-p^i}{1-p^M},\ j=0,1,2\ldots.M,$$

$$x_j = = \frac{-\bar{x}(j)-\bar{x}(j-1)}{p^M-1},\ \text{where } j=1,2\ldots.M,$$

Grid formation for q-mesh is defined as

- Set $N' = \frac{N}{2}$ and $\sigma = \frac{5-\varepsilon}{5N'}$, where $N = 2^J$(J: Maximum resolution level).
- Evaluate $\delta = \frac{1-2\sigma N'}{(-2N'+1)N'}$.

- Specify the grid points as $t'_0 = 0, t'_i = -\delta + i\sigma - \delta\frac{i(i-1)}{2}$,i:1,2...,2N'.
- Set $\overline{t_0} = 0,\ \overline{t_i} = \frac{1}{2}(-t'_{2N'-i} + 1)$ where i:1, 2...,2N'.
- In similar manner, set $\bar{t} = -t'_{4M'-i} + 1$, i: 1+2N',2+2N',...,4N'.
- Lastly, define the collocation points as using these grid points $t_i = \frac{\overline{t_{i-1}} + \overline{t_i}}{2}$.

Table 7: Table of Maximum absolute residual errors on the Shishkin-mesh for different values of ε calculated by the uniform Haar wavelet method.

ε	$J_{16}(x_j)$	$J_{32}(x_j)$	$J_{64}(x_j)$	$J_{128}(x_j)$	$J_{256}(x_j)$	$J_{512}(x_j)$	$J_{1024}(x_j)$
2^{-2}	1.9516e−16	3.8511e−16	4.3238e−16	8.7473e−16	1.0632e−15	1.5339e−15	2.4865e−15
2^{-6}	1.2197e−17	2.4069e−17	2.7024e−17	5.4671e−17	6.6451e−17	9.5807e−17	1.5541e−16
2^{-10}	5.9631e−19	7.6233e−19	1.5043e−18	1.6890e−18	3.4169e−18	4.1532e−18	9.7128e−18
2^{-14}	4.7646e−20	9.4021e−20	1.0556e−19	2.1356e−19	2.5958e−19	3.7448e−19	6.0705e−19
2^{-18}	2.9779e−21	5.8763e−21	6.5970e−21	1.3347e−20	1.6223e−20	2.3405e−20	3.7941e−20
2^{-22}	3.6467e−14	3.7366e−14	3.7595e−14	3.7653e−14	3.7667e−14	3.7667e−14	3.7671e−14
2^{-26}	2.2792e−15	2.3354e−15	2.3497e−15	2.2533e−15	2.3542e−15	2.3542e−15	2.3545e−15
2^{-30}	1.4245e−16	1.4596e−16	1.4686e−16	1.4708e−16	1.4714e−16	1.4714e−16	1.4715e−16
2^{-34}	8.9030e−18	8.9030e−18	9.1226e−18	9.1785e−18	9.1925e−18	9.1969e−18	9.1971e−18
2^{-38}	1.0028e−14	1.0080e−14	1.0093e−14	1.0097e−14	1.0097e−14	1.0097e −14	1.0098e−14
2^{-42}	3.9039e−14	39043e−14	3.9044e−14	3.9044e−14	3.9044e−14	3.9044e−14	3.9044e−14
2^{-46}	1.0621e−14	1.0616e−14	1.0614e−14	1.0614e−14	1.0614e−14	1.0614e−14	1.0641e−14
2^{-50}	6.6381e−16	6.6348e−16	6.6339e−16	6.6337e−16	6.6336e−16	6.6336e−16	6.6336e−16

2^{-54}	4.1488e−17	4.1467e−17	4.1462e−17	4.1461e−17	4.1460e−17	4.1460e−17
4.1460e−17						

For problem 2, Table-7 illustrates the maximum absolute residual error by the numerical algorithm applied with the UHWM on Shishkin mesh with different values of perturbation parameter (ε) and level of resolution (J). From the Table-7, it can be seen that present method works effectively while increasing the grid points in the method. Table-7 draw a conclusion that, on Shishkin mesh the uniform Haar wavelet scheme performs very well for small values of perturbation parameter (ε). In compared to other methods, such as the parameter uniform technique and the non-uniform HWM, the uniform Haar wavelet method's accuracy increases.

Table 8: Non-uniform Haar wavelet method on Shishkin-mesh, the calculation of maximum absolute residual errors for various values of ε.

ε	$J_{32}(x_j)$	$J_{64}(x_j)$	$J_{128}(x_j)$	$J_{256}(x_j)$	$J_{512}(x_j)$	$J_{1024}(x_j)$
2^{-2}	1.5543e−14	8.8818e−15	9.3259e−15	9.7700e−15	3.4639e−14	3.2863e−14
2^{-6}	1.5099e−14	1.0658e−14	1.1102e−14	9.7700e−15	3.7303e−14	3.4639e−14
2^{-10}	3.3751e−14	3.2863e−14	1.4655e−14	1.9096e−14	2.8422e−14	1.3323e−14
2^{-14}	1.7764e−14	1.4566e−14	2.7089e−14	1.4211e−14	2.4869e−14	1.4211e−14
2^{-18}	1.8652e−14	3.7748e−14	1.7764e−14	4.3077e−14	2.3981e−14	5.3291e−14
2^{-22}	2.5313e−14	1.2434e−14	2.9310e−14	4.1744e−14	3.3307e−14	3.9524e−14
2^{-26}	1.9096e−14	1.1990e−14	3.7303e−14	3.4195e−14	3.9524e−14	2.6201e−14
2^{-30}	1.9540e−14	1.1102e−14	4.0412e−14	1.3767e−14	2.8422e−14	4.8400e−14
2^{-34}	2.4869e−14	1.2434e−14	3.5971e−14	1.2434e−14	3.1086e−14	2.4869e−14
2^{-38}	2.0428e−14	1.1990e−14	3.8636e−14	1.2434e−14	2.9310e−14	2.3093e−14
2^{-42}	2.3093e−14	1.0658e−14	3.5971e−14	1.2434e−14	2.0428e−14	4.4853e−14
2^{-46}	2.1760e−14	1.1102e−14	3.3307e−14	1.2434e−14	2.9310e−14	2.3093e−14
2^{-50}	2.2204e−14	1.1990e−14	3.6859e−14	1.2434e−14	2.5313e−14	4.6185e−14

Table-8 presents the maximum absolute residual errors obtained by non-uniform HWM on Shishkin mesh for various values of perturbation parameter (ε). And different values of grid

points in the numerical method of non-uniform Haar wavelet method. Maximum absolute residual errors have been tabulated for different increasing resolution level (J) and decreasing perturbation parameter (ε). The results of maximum absolute residual error of UHWM as given in Table-7 is very effective for various ε such as $\varepsilon = 2^{-18}$ on Shishkin mesh as the residual error is improved then the residual error produced in non-uniform HWM is given in Table-8.

Table 9 Parameter uniform method on Shishkin-mesh, the calculation of maximum absolute residual errors for various values of perturbation parameter (ε) and resolution level (J).

ε	$J_{08}(x_j)$	$J_{16}(x_j)$	$J_{32}(x_j)$	$J_{64}(x_j)$	$J_{128}(x_j)$	$J_{256}(x_j)$
2^{0}	2.6110e−03	6.5500e−04	1.6440e−04	4.1100e−05	1.0270e−05	2.5670e−06
2^{-2}	2.5760e−03	6.4630e−04	1.6170e−04	4.0440e−05	1.0110e−05	2.5260e−06
2^{-4}	2.7920e−03	7.0150e−04	1.7660e−04	4.4170e−05	1.1040e−05	2.7580e−06
2^{-6}	2.9200e−03	7.2900e−03	1.8240e−04	4.5620e−05	1.1410e−05	2.8490e−06
2^{-8}	3.0350e−03	7.5260e−04	1.8830e−04	4.7070e−05	1.1770e−05	2.9390e−06
2^{-10}	3.1160e−03	7.8060e−04	1.9390e−04	4.8420e−05	1.2300e−05	3.0550e−06
2^{-12}	3.1520e−03	7.9670e−04	1.9810e−04	4.9350e−05	1.2300e−05	3.0550e−06
2^{-14}	24869e−04	1.2434e−04	3.1630e−03	8.0310e−04	2.0040e−04	4.9930e−05
2^{-16}	3.1670e−03	8.0520e−04	2.0120e−04	5.0210e−05	1.2520e−05	3.1130e−06
2^{-18}	3.1680e−03	8.0570e−04	2.0150e−04	5.0320e−05	1.2550−05	3.1240e−06
2^{-20}	3.1680e−03	8.0590e−04	2.0160e−04	5.0370e−05	1.2570e−05	3.1330e−06
2^{-22}	3.1680e−03	8.0590e−04	2.0160e−04	5.0370e−15	1.2580e−05	3.1350e−06
2^{-24}	3.1680e−03	8.0590e−04	2.0160e−04	5.0380e−05	1.2580e−05	3.1360e−06
2^{-26}	3.1680e−03	8.0590e−04	2.0160e−04	5.0370e−05	1.2550e−05	3.0960e−06
2^{-28}	3.1680e−03	8.0590e−04	2.0160e−04	5.0380e−05	1.2560e−05	3.1120e−06

Table-9 shows the maximum absolute residual errors obtained by parameter uniform method on Shishkin mesh for various values of ε and J. The maximum absolute residual errors decrease as the values of resolution level in the parameter uniform approach increase and perturbation parameter values decrease. In addition, Table-7 and Table-9 provide the findings of the

maximum absolute residual errors generated by UHWM. For a range of perturbation parameter values (ε), the UHWM performs exceptionally well such as $\varepsilon = 2^{-18}$ based on the findings of the parameter uniform technique as shown in Table 9 on the Shishkin mesh.

Table 10: Maximum absolute residual errors obtained by uniform Haar wavelet method on q-mesh for various values of ε.

ε	$J_{16}(x_j)$	$J_{32}(x_j)$	$J_{64}(x_j)$	$J_{128}(x_j)$	$J_{256}(x_j)$	$J_{512}(x_j)$	$J_{1024}(x_j)$
2^{-2}	3.4694e−18	3.4694e−18	8.6736e−19	8.6736e−19	1.3010e−18	0	0
2^{-6}	2.1684e−19	2.1684e−19	5.4210e−20	5.42101e−20	8.1315e−20	0	0
2^{-10}	1. 3553e−20	1.3553e−20	3.3881e−21	3.3881e−21	5.0822e−21	0	0
2^{-14}	8.4703e−22	8.4703e−22	2.1176e−22	2.1176e−22	3.1764e−22	0	0
2^{-18}	5.2940e−23	5.2940e−23	1.3235e−23	1.3235e−23	1.9852e−23	0	0
2^{-22}	1.9852e−23	2.6470e−23	8.2718e−25	1.6544e−25	1.2408e-24	8.2718e−25	8.2718e−25
2^{-26}	1.2408e−24	1.6544e−24	5.1699e−26	1.0340e−25	7.7548e−26	5.1699e−25	5.1699e−26
2^{-30}	7.7548e−26	1.0340e−25	3.2312e−27	6.4623e−27	4.8468e−27	3.2312e−27	3.2312e−27
2^{-34}	4.8468e−27	6.4623e−27	2.0195e−28	4.0390e−28	3.0292e−28	2.0195e−28	2.0195e−28
2^{-38}	5.6372e−22	1.3538e−24	4.5817e−27	2.0195e−28	2.2404e−28	1.6408e −28	4.8909e−29
2^{-42}	2.0153e−16	4.1497e−17	5.4130e−18	6.9071e−19	8.7217e−20	1.0957e−20	1.3730e−21
2^{-46}	3.2097e−16	1.3831e−16	6.3955e−17	3.0719e−17	1.5050e−17	7.4482e−18	3.7050e−18
2^{-50}	2.0061e−17	8.6443e−18	3.9972e−18	1.9119e−18	9.4062e−19	4.6551e−19	2.3156e−19
2^{-54}	1. 2538e−18	5.4027e−19	2.4982e−19	1.200e−19	5.8789e−20	2.9095e−20	4.1460e−20

On Shishkin mesh and q-mesh, Tables 7 and 10 compare the maximum absolute residual errors produced by the uniform Haar wavelet method. When using different values of the perturbation parameter, the uniform Haar wavelet approach compares its results with those produced using the parameter uniform method and the non-uniform Haar wavelet method.

The outcomes of Problem 2 concur with the theoretical findings presented in Section 3 of this article. These conclusions were reached using various perturbation parameter values and J resolution levels. Authors found that the uniform Haar wavelet-based approach is more accurate and fast converges when compared the highest absolute residual error on Shishkin mesh and q-mesh, which is presented in Tables 7 and 10, with the residual errors caused by current methods, which are given in Tables 8, 9, and 11.

Table 11: Maximum absolute residual errors obtained by non-uniform Haar wavelet method on q-mesh for various values of ε.

ε	$J_{16}(x_j)$	$J_{32}(x_j)$	$J_{64}(x_j)$	$J_{128}(x_j)$	$J_{256}(x_j)$	$J_{512}(x_j)$ $J_{1024}(x_j)$
2^{-6}	5.3291e−15	4.4409e−15	7.1054e−15	5.7732e−15	8.4377e−15	3.3751e−14
2^{-10}	5.3291e−15	3.9968e−15	6.6613e−15	5.7732e−15	8.4377e−15	3.4639e−14
2^{-14}	5.3291e−15	3.5527e−15	7.1054e−15	5.3291e−15	8.8818e−15	3.5083e−14
2^{-18}	5.3291e−15	4.4409e−15	7.1054e−15	5.3291e−15	8.8818e−15	3.5083e−14
2^{-22}	5.3291e−15	4.4409e−15	7.1054e−15	5.7732e−15	8.8818e−15	3.5083e−14
2^{-26}	5.3291e−15	4.4409e−15	7.1054e−15	5.7732e−15	8.8818e−15	3.6415e−14
2^{-30}	5.3291e−15	4.4409e−15	7.1054e−15	6.2172e−15	8.8818e−15	3.5971e−14
2^{-34}	5.3291e−15	3.9968e−15	7.1054e−15	5.7732e−15	8.8818e−15	3.5527e−14
2^{-38}	5.3291e−15	3.9968e−15	6.6613e−15	5.7732e−15	8.8818e−15	3.5527e−14
2^{-42}	5.3291e−15	3.9968e−15	6.6613e−15	5.7732e−15	8.8818e−15	3.5083e−14
2^{-46}	5.3291e−15	4.4409e−15	7.1054e−15	5.7732e−15	8.8818e−15	3.5083e−14
2^{-50}	4.8850e−15	3.9968e−15	6.6613e−15	5.7732e−15	8.8818e−15	3.5083e−14

Table-10 illustrates the maximum absolute residual error obtained by uniform Haar wavelet method on q-mesh for various values of perturbation parameter and level of resolution. Table-10 shows that, on increasing the grid points in the uniform Haar wavelet method, the maximum absolute residual error decreases. Tables 10 and 11 show that, for specific values of ε (2^{-34}) the maximum absolute residual errors are more stabilized when compared to the non-uniform Haar wavelet approach with q-mesh. Table-10 clearly demonstrates the uniform convergence of the current scheme.

In their analysis of the Haar solution for Shishkin mesh and q-mesh, the authors come to the conclusion that the obtained maximum residual errors represent the increased accuracy. As can be seen from Tables 7 and 10, the maximum absolute residual error is higher close to the transition points than it is in the rest of the domain.

Authors conclude that, the greatest absolute residual error for Shishkin mesh is 8.9030e-18 for ε= 2^{-34} and J=16. On q-mesh, however, it will be 4.8468e-27 for the same perturbation parameter value. Therefore, for Problem 2, the uniform Haar wavelet scheme converges on the q-mesh faster than the Shishkin-mesh.

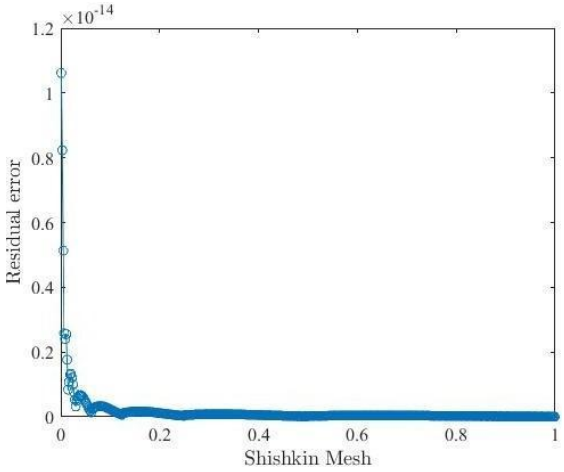

Fig.16: Residual error for ε = $\frac{1}{2^{46}}$, J=8 on Shishkin-mesh.

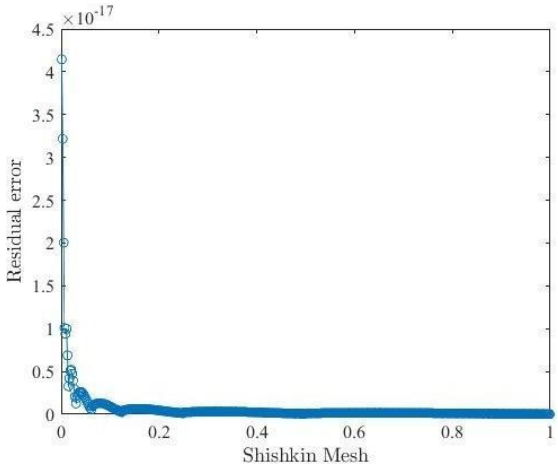

Fig.17: Residual error for ε = $\frac{1}{2^{54}}$, J=8 on Shishkin-mesh.

For Problem 2, the maximum absolute residual error on Shishkin mesh caused by calculating the numerical algorithm described in Section 5. In addition, a graph of the maximum residual error in uniform Haar wavelet solution is shown in Fig.16 and Fig.17 with residual error 1.1978e−14

and 4.1573e−17 for J = 8 and perturbation parameter $\varepsilon = \frac{1}{2^{46}}$ and $\varepsilon = \frac{1}{2^{54}}$. To plot graphs (Fig.: 16-17), authors take $\varepsilon = \frac{1}{2^{46}}$, and $\varepsilon = \frac{1}{2^{54}}$ with J=8 and draw the conclusion that, on decreasing the value of ε, the maximum residual error decrease for Shishkin mesh.

7 Conclusion

In the current study, uniform Haar wavelet scheme has been used on various meshes, including Shishkin mesh, p-mesh, and q-mesh to solve the system of partially singularly perturbed initial and boundary value problems. In fact, the maximum absolute residual error occurred, and tabulated for non-uniform grid. Furthermore, figures 1–10 clearly demonstrate that the Haar wavelet is uniform on non-uniform grid points. Accuracy, convergence of the present scheme for small values of perturbation parameter ε as well as computational complexity are the major research gaps with the existing schemes. Improvement on accuracy, convergence of the present scheme for small values of perturbation parameter ε as well as computational complexity of the uniform Haar wavelet scheme has been carried out by performing the simulation on different mesh to bridge the gap in error analysis as given in section-5. The present method approximates the numerical solution of system of partially singularly perturbed initial (first-order) and boundary value problems (second order) on a non-uniform grid. The uniform Haar wavelet method limited to the strong and weak variation of the perturbation parameter ε that affects the boundary layer width and the uniform Haar solutions. Thus, care should be used while selecting the transition parameters. The proposed scheme provides the better approximation with less computational cost then the non-uniform Haar wavelet method, parameter uniform method and finite difference operator method: it is due to the sparsity of the transition matrix and small Haar wavelet coefficients. It is worth mentioning that uniform Haar wavelet method provides excellent results for small and large values of perturbation parameter. In light of this, uniform Haar wavelet method is quite effective for solving partially singularly perturbed initial and boundary value problems numerically. Additionally, the uniform Haar wavelet method has been applied directly on all type of differential equations, linear or non-linear, homogeneous or non-homogeneous either constant coefficient or with variable coefficients directly. Further, the

proposed method can used to resolve partially singularly perturbed initial and boundary value problems that are parabolic, hyperbolic, nonlinear and also for the fractional differential equations that involves in various physical applications specially in theoretical analysis for the future research work. The technique introduced here is easy to apply as well as yields more accurate results.

Nomenclature:

UHWM: Uniform Haar Wavelet Method.

SPIVP: Singularly Perturbed Initial Value Problem.

ε: Small perturbation parameter.

ϑ_i, $i = 1, 2, 3$: End points of the sub-intervals.

α_i, $i = 1, 2, 3$: Constant coefficients.

u_i, $i = 1, 2, 3, 4$: Real valued continuous functions.

$r_1(x)$, $r_2(x)$: Arbitrary functions.

ρ_x: Transitional parameter.

$H_i^w(x)$: Haar wavelet function.

J: Highest level of resolution.

j: Resolution level at various levels.

m: Representation of scaling parameter.

M: Fixed finite number.

k: Parameter of translation.

i: Index of Haar function.

$P^w_{i,\varsigma}$: Haar operational matrix.

a_i, $i = 1, 2 \ldots, 2M$ Haar coefficient.

q_i^1, q_i^1: Uniform Haar wavelet coefficients.

$\delta_{i,\bar{i}}$: Kronecker delta.

ODE: Ordinary Differential Equation.

HWM: Haar Wavelet Method.

Φ: Unknown function.

s: Space variable.

t: Time variable.

μ_i: Constant parameter, i=1.

$H_i(s)$: Haar wavelet function.

a, ς_1, ς_2, ς_3, ς_4, b: Some real numbers.

C: Integral of $P^w_{i,1}$ from a to b.

λ_i: Unknown Haar wavelet coefficients.

i:$\sqrt{-1}$.

X_l: Collocation points.

δ_t: Time discretizing unit.

$\Phi_M(x, \tau)$: Haar wavelet representation of Φ.

E_r: Error term due to Haar wavelet approximation.

P: Positive number.

Declaration:

Conflict of Interest: There are no conflicts of interest declared by the authors.

Data availability statement: Data sharing not applicable to this paper as no datasets were created or processed during the current study.

Acknowledgement:

I would like to express my sincere thanks to Late Professor Manoj Kumar, Department of Mathematics, MNNIT Allahabad, for serving as my study's most important inspiration. I am grateful for his suggestions, support, and help.

References

Ahsan, M., Bohner, M., Ullah, A., Khan, A.A. and Ahmad, S. (2023) "A Haar wavelet multi resolution collocation method for singularly perturbed differential equations with integral boundary conditions", Mathematics and Computers in Simulation Vol. 204, pp. 166-180.

Cengizci, S., Kumar, D., Atay, M. (2023),"Semi-Analytic Method for Solving Singularly Perturbed Twin-Layer Problems with a Turning Point", Mathematical Modelling and Analysis, Vol. 28, No. 1, pp. 102–117.

Chen, C.F. and Hsiao, C.H. (1997), "Haar wavelet method for solving lumped and distributed parameter systems", IEE Proceedings - Control Theory and Applications, Vol. 144, No. 1, 87-94.

Clavero, C. and Jorge, J.C. (2016) “Uniform convergence and order reduction of the fractional implicit Euler method to solve singularly perturbed 2D reaction-diffusion problems”, Applied Mathematics and Computation, Vol. 287-288, pp. 12-27.

Das, P. and Natesan, S. (2004) "Optimal error estimate using mesh equidistributional technique for singularly perturbed system of reaction-diffusion boundary-value problems", Applied Mathematics and Computation, Vol. 249, pp.265-277.

Das, P. and Aguiar, J.V. (2017), "Parameter uniform optimal order numerical approximation of a class of singularly perturbed system of reaction diffusion problems involving a small perturbation parameter", Journal of Computational and Applied Mathematics, Vol. 24, No. 3.

Kumar, D., and Deswal, K. (2021) "Wavelet-based approximation for two-parameter singularly perturbed problems with Robin boundary conditions", Journal of Applied Mathematics and Computing, Vol. 68, pp. 125-149.

Deswal, K., Kumar, D. and Aguiar, J.V. (2022), "Three-dimensional Haar wavelet method for singularly perturbed elliptic boundary value problems on non-uniform meshes", Journal of Mathematical Chemistry, Vol. 60 pp. 1314-1336.

Doolan, E. P., Miller, J. J. H. and Schillers, W. H. A., (1980), "Uniform Numerical Methods for Problem with Initial and Boundary Layers" Boole Press.

Hsiao, C.H. (1997), "State analysis of the linear time delayed systems via Haar wavelets", Mathematics and Computers in Simulation Vol. 44, No. 5, pp. 457-470.

Islam, S., Aziz, I. and Sarler, B. (2010), "The numerical solution of second order boundary value problems by collocation method with Haar wavelets", Mathematical and Computer Modelling, Vol. 50, pp. 1577-1590.

Lambert, J.D. (1991), "Numerical Methods for Ordinary Differential Equations", Wiley, Chichester.

Lepik, U. (2011), "Solving PDEs with the aid of two-dimensional Haar wavelets", Computers and Mathematics with Applications Vol. 61, pp. 1873-1879.

Lepik, U and Hein, H. (2014), "Haar Wavelets Applications" (Springer International Publishing, Switzerland.

Lepik, U. (2008), "Solving integral and differential equations by the aid of non-uniform Haar wavelets", Applied Mathematics and Computation, Vol. 198, pp. 326-332.

Liu, L., Ahsan, M., Ahmad, M., Nisar, M., Liu, X., Ahmad, I., and Ahmad, H. (2021) "Applications of Haar wavelet-finite difference hybrid method and its convergence for hyperbolic nonlinear Schrödinger equation with energy and mass conversion", Energies Vol. 14, No. 23.

Matthews, S. (2000) "parameter robust numerical methods for a system of two coupled singularly perturbed reaction diffusion equations", Master Thesis, School of Mathematical Sciences, Dublin City University.

Majak, J., Shvartsman, B., Kirs, M., Pohlak, M., and Herranen, H. (2015) Convergence theorem for the Haar wavelet-based discretization method Compos. Struct. Vol. 126 pp. 227–232.

Mandel Zweig, V.B. and Tabakin, F. (2001), "Quasi linearization approach to nonlinear problems in physics with application to nonlinear ODEs", Computer Physics Communications. Vol. 141 No. 2, pp. 268-281.

Matthews, S., O'Riordan, E. and Shishkin, G.I. (2002) "A numerical method for a system of singularly perturbed reaction-diffusion equations", Journal of Computational and Applied Mathematics, Vol.145, pp. 151-166.

Mallat, S.G. (1989) "Multiresolution approximations and wavelet orthonormal bases of L^2(R)", Transactions of the American Mathematical Society, Vol. 315, pp. 69-87.

Matthews, S., O'Riordan, E. and Shishkin, G.I. (2006), "A numerical method for a system of singularly perturbed reaction-diffusion equations Journal of Computational and Applied Mathematics" Vol. 145, pp. 151-166.

Matthews, S., O'Riordan, E. and Shishkin, G.I. (1996), "Fitted numerical methods for singular perturbation problems", world Scientific, Singapore.

Meenakshi, M.P., Valarmathi, S. and Miller, J.J.H. (2010), "Solving a partially singularly perturbed initial value problem on Shishkin meshes", Applied Mathematics and Computation, Vol.215, pp. 3170- 3180.

O'Riordan, E. and Stynes, M. (1986), "A uniformly accurate Finite-element method for a singularly perturbed one-dimensional reaction-diffusion problem", Mathematics of Computation, Vol. 47, No.176, pp. 555–570.

Pandit, S. and Kumar, M. (2012), "Wavelet Transform and Wavelet-based Numerical Methods", International Journal of Nonlinear Science, Vol. 13, pp. 325-345.

Qureshi, S., Soomro, A., Hincal, E., Lee, J.R., Park, C., Osman, M.S. (2022), "An efficient variable step size rational method for stiff, singular and singularly perturbed problems", Alexandria Engineering Journal, Vol. 61(12), pp. 10953-10963.

Raza, A. and Khan, A. (2019), "Haar Wavelet series solution for solving neutral delay differential equations", Journal of King Saud University-Science, Vol. 31, pp. 1070-1076.

Raza, A. and Khan, A. (2021), "Solution of Partially Singularly Perturbed System of Initial and Boundary Value Problems Using Non-Uniform Haar Wavelet", TWMS Journal of Applied and Engineering Mathematics, Vol. 11, No.4, pp. 1246-1259.

Roos., H.G., Stynes, M. and Tobiska, L. (1996), "Numerical methods for singularly perturbed differential equations", Springer-Verlag.

Roos, H.G., Stynes, M. and Tobiska, L. (2008), "Robust Numerical Methods for Singularly Perturbed Differential Equations, Springer Series in Computational Mathematics", Springer Series in Computational Mathematics, Vol. 24.

Sahoo, S.K., and Gupta, V. (2023), "A robust uniformly convergent finite difference scheme for the time-fractional singularly perturbed convection-diffusion problem", Computers & Mathematics with Applications, Vol. 137, pp. 129-146.

Shishkin, G.I. (1988), "A difference scheme for a singularly perturbed equation of parabolic type with a discontinuous boundary condition", Mat. Fiz., Vol. 28, pp. 1649-1662.

Singh, R., Garg, H., and Galería, V. (2019), "Haar wavelet collocation method for Lane–Emden equations with Dirichlet, Neumann and Neumann–Robin boundary Conditions", Journal of Computational and Applied Mathematics Vol. 346, pp. 150-161.

Singh, S., Kumar, D., Shanthi, V., (2023) “Uniformly convergent scheme for fourth-order singularly perturbed convection-diffusion ODE”, Applied Numerical Mathematics, Vol. 186, pp. 334-357.

Simos, T.E., and Famelis, I.T. (2022)," A neural network training algorithm for singular perturbation boundary value problems", Neural Computing and Applications, Vol. 34, pp. 607–615.

Swati, Singh, K., Verma, A.K., Singh, M. (2020), "Higher order Emden–Fowler type equations via uniform Haar Wavelet resolution technique", Journal of Computational and Applied Mathematics Vol. 376.

Umesh, and Kumar, M. (2021), "Numerical solution of Lane-Emden type equations using Adomian- decomposition method with unequal step-size partitions", Engineering Computations, Vol. 38, pp. 1-18.

Valarmathi, S. and Miller, J.J.H. (2009), "A parameter-uniform finite difference method for a singularly perturbed initial value problem: a special case", Lecture notes in Computational Science and Engineering, Vol. 29, Springer-Verlag, pp. 267–276.

Wichailukkana, N., Novaprateep, B., and Boonyasiriwat, C. (2016) "A convergence analysis of the numerical solution of boundary-value problems by using two-dimensional Haar wavelets", Science Asia Vol. 42, pp. 346-355.

Xu, Z., Xu, L., Li. W., Shi, S. (2023), "Renormalization Group Method for Singular Perturbation Initial Value Problems with Delays", Mediterranean Journal of Mathematics Vol. 20.

Zhang, J., Xiaoqi, M., and Liv, V. (2021) "Finite element method on Shishkin mesh for a singularly perturbated problems with an interior layer", Applied Mathematics Letters, Vol. 121.